

# Synthesis, crystal structure, and thermal decomposition kinetics of complex $[\text{Nd}(\text{BA})_3\text{bipy}]_2$

H. M. Ye · N. Ren · H. Li · J. J. Zhang ·  
S. J. Sun · L. Tian

Received: 25 June 2009 / Accepted: 17 August 2009 / Published online: 19 September 2009  
© Akadémiai Kiadó, Budapest, Hungary 2009

**Abstract** The complex of  $[\text{Nd}(\text{BA})_3\text{bipy}]_2$  (BA = benzoic acid; bipy = 2,2'-bipyridine) has been synthesized and characterized by elemental analysis, IR spectra, single crystal X-ray diffraction, and TG/DTG techniques. The crystal is monoclinic with space group  $P2(1)/n$ . The two-eight coordinated  $\text{Nd}^{3+}$  ions are linked together by four bridged BA ligands and each  $\text{Nd}^{3+}$  ion is further bonded to one chelated bidentate BA ligand and one 2,2'-bipyridine molecule. The thermal decomposition process of the title complex was discussed by TG/DTG and IR techniques. The non-isothermal kinetics was investigated by using double equal-double step method. The kinetic equation for the first stage can be expressed as  $dx/dt = A \exp(-E/RT)(1 - \alpha)$ . The thermodynamic parameters ( $\Delta H^\ddagger$ ,  $\Delta G^\ddagger$ , and  $\Delta S^\ddagger$ ) and kinetic parameters (activation energy  $E$  and pre-exponential factor  $A$ ) were also calculated.

**Keywords** Benzoic acid · Crystal structure · TG/DTG · Non-isothermal kinetics

## Introduction

The synthesis of lanthanide carboxylate complexes has been a field of rapid growth because of the interesting structures [1–5] and potential applications, such as light conversion molecular devices (LCMD) [6], functional probes in biological systems [7], and so on [8]. So far, the thermal behavior about lanthanide complexes has been also widely reported [9–19]. In this paper, a new crystal structure of  $[\text{Nd}(\text{BA})_3\text{bipy}]_2$  was obtained. The thermal decomposition process of the title complex was determined by TG/DTG technique and the nonisothermal kinetics was studied by using the double equal-double step method [20].

## Experimental section

### Chemicals and apparatus

$\text{Nd}_2\text{O}_3$  ( $\geq 99.99\%$ ), benzoic acid, and 2,2'-bipyridine were obtained from commercial sources. Elemental analysis (C, H, N) was determined on a Flash EA 1112 element analyzer, and the metal content was assayed using EDTA titration method. IR spectra were recorded at room temperature from 4,000 to  $400 \text{ cm}^{-1}$  on a Perkin-Elmer FTIR-1730 spectrometer by using the KBr pellets. The molar conductance was determined with a Shanghai DDS-307 conductivity meter. The single crystal X-ray diffraction data were obtained by Saturn 724+ diffractometer. TG/DTG experiments were operated on Perkin-Elmer TGA7 thermogravimetric analyzer, and the heating rate was (3, 5, 10, 12, and 15)  $\text{K min}^{-1}$  from 298.15 to 1223.15 K with a static atmosphere.

---

H. M. Ye · J. J. Zhang (✉) · S. J. Sun · L. Tian  
Experimental Center, Hebei Normal University,  
Shijiazhuang 050016, People's Republic of China  
e-mail: jjzhang6@126.com

H. M. Ye · S. J. Sun · L. Tian  
College of Chemistry and Material Science, Hebei Normal  
University, Shijiazhuang 050016, People's Republic of China

N. Ren  
Department of Chemistry, Handan College, Handan 056005,  
People's Republic of China

H. Li  
Shijiazhuang College, Shijiazhuang 050035,  
People's Republic of China

## Synthesis of [Nd(BA)<sub>3</sub>bipy]<sub>2</sub>

Benzoic acid (0.6 mmol) and 2,2'-bipyridine (0.2 mmol) were mixed and dissolved in 95% C<sub>2</sub>H<sub>5</sub>OH solution. The pH value of the mixed solution was adjusted to 6–7 with NaOH(1 mol L<sup>-1</sup>) solution and then added the ligands to NdCl<sub>3</sub>·6H<sub>2</sub>O (0.2 mmol) solution in dropwise with stirring for 8 h. After deposited for 12 h, the precipitates were filtered out and purple crystals were obtained by slow evaporation of the mother solution at room temperature after 3 weeks.

## X-ray diffraction determination

A single crystal of [Nd(BA)<sub>3</sub>bipy]<sub>2</sub> with dimensions 0.37 × 0.30 × 0.30 mm<sup>3</sup> was used for the structure determination. Data were collected on a Saturn 724+ diffractometer with graphite-monochromated Mo K $\alpha$  radiation ( $\lambda = 0.71073 \text{ \AA}$ ) at 293(2) K in the range of  $3.03^\circ \leq \theta \leq 27.49^\circ$  with multi-scan technique. The structure was solved by direct methods using SHELXS-97 program and refined by Full-matrix least-squares on  $F^2$  using SHELXL-97 program to  $R_1 = 0.0289$ ,  $wR_2 = 0.0683$ .

## Results and discussion

### Elemental analysis and molar conductivity

The content of C, H, N, Nd, and molar conductivity of the title complex are listed in Table 1. The experiment data of the elemental analysis are consistent well with the theoretical values. And it can be concluded that the title complex is a nonelectrolyte from the molar conductivity value.

**Table 1** Elemental analysis and molar conductivity for [Nd(BA)<sub>3</sub>bipy]<sub>2</sub>

[Nd(BA) <sub>3</sub> bipy] <sub>2</sub>	C/%	H/%	N/%	Nd/%	$\Lambda/S/cm^2 \text{ mol}^{-1}$
Found	55.95	3.56	4.42	21.96	19.66
Calcd	56.09	3.49	4.22	21.73	–

**Table 2** IR data for the ligands and complex (cm<sup>-1</sup>)

Compounds	$\nu_{C=N}$	$\delta_{C-H}$	$\nu_{C=O}$	$\nu_{as}(COO^-)$	$\nu_s(COO^-)$	$\nu(Nd-O)$
bipy	1578	992,757	–	–	–	–
HBA	–	–	1688	–	–	–
[Nd(BA) <sub>3</sub> bipy] <sub>2</sub>	1597	1012,764	–	1627	1407	425

The crystal is purple and can exist stably at room temperature in air. It is insoluble in water, ethanol, and acetone solution, but it is freely soluble in DMSO and DMF solution.

## Infrared spectra

The characteristic absorption of the ligands and complex in IR spectra are listed in Table 2. The characteristic absorption of  $\nu_{C=O}$  (COOH, 1688 cm<sup>-1</sup>) disappears, meanwhile two new absorption bands ascribed to the carboxylate group (COO<sup>-</sup>),  $\nu_{as}$  (1627 cm<sup>-1</sup>) and  $\nu_s$  (1,407 cm<sup>-1</sup>) appear in the spectra of the title complex. These indicate that the oxygen atoms of benzoic acid are coordinated to the Nd<sup>3+</sup> ion [21]. Furthermore, the appearance of  $\nu_{Nd-O}$  (425 cm<sup>-1</sup>) also indicates that the oxygen atoms of the carboxylate group are coordinated to the Nd<sup>3+</sup> ion. At the same time, the bands of  $\nu_{CN}$  (1578 cm<sup>-1</sup>),  $\delta_{CH}$  (992 cm<sup>-1</sup>, 757 cm<sup>-1</sup>) of bipy ligand shift to higher values around at (1597, 1012, and 764) cm<sup>-1</sup>, indicating that the chemical bonds are formed between Nd<sup>3+</sup> ion and nitrogen atoms of bipy [22, 23].

## Structure description of [Nd(BA)<sub>3</sub>bipy]<sub>2</sub>

Crystallographic data for the title complex are presented in Table 3 and the selected bond lengths and angles are listed in Table 4. The structure of the title complex is shown in Fig. 1, which shows that the Nd<sup>3+</sup> ion is coordinated by two oxygen atoms from one bidentate chelating carboxylic group, four oxygen atoms from four bridging bidentate carboxylic groups, and two nitrogen atoms from one bipy molecule, giving a coordination number of eight. The two Nd<sup>3+</sup> ions are linked together by four bridging bidentate carboxylic ligands. The coordination mode is the same as [Ln(BA)<sub>3</sub>bipy]<sub>2</sub> (Ln = Sm, Dy, and Eu) [24–26]. And Fig. 2 shows the coordination polyhedron around Nd<sup>3+</sup> is trigondodecahedron.

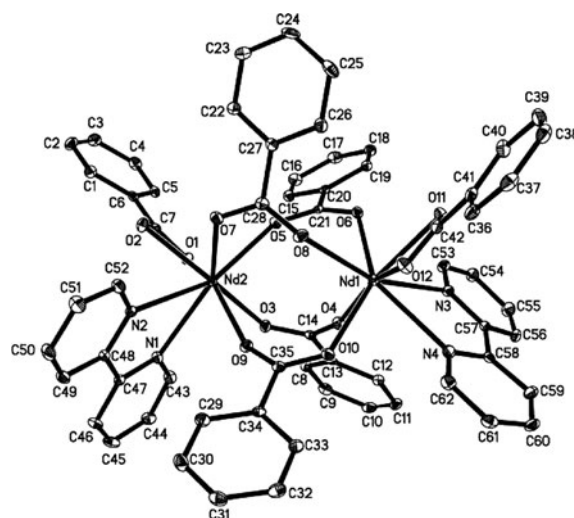
The length of Nd–O bonds is in the range of 2.3615(19)–2.5013(19) Å, with an average length of 2.4314(19) Å. The Nd–O bond distances formed by the bridging bidentate BA groups are slightly shorter than that formed by the bidentate chelating BA groups due to instability of four-membered ring in the chelating mode [27]. The Nd1–N distances range from 2.640(2) to 2.673(2) Å, with an average value of 2.657(2) Å. So the length of Nd–N bonds is longer than

**Table 3** Crystal data and structure refinement for the title complex

Empirical formula	C <sub>62</sub> H <sub>46</sub> N <sub>4</sub> Nd <sub>2</sub> O <sub>12</sub>
Formula weight	1327.51
Temperature	293(2) K
Wavelength	0.71073 Å
Crystal system, space group	Monoclinic, <i>P2(1)/n</i>
Unit cell dimensions	$a = 14.1282(13)$ Å $\alpha = 90^\circ$ $b = 15.2529(13)$ Å $\beta = 103.5530(10)^\circ$ $c = 25.969(2)$ Å $\gamma = 90^\circ$
Volume	$5440.5(8)$ Å <sup>3</sup>
Z, Calculated density	4, 1.621 Mg m <sup>-3</sup>
Absorption coefficient	1.956 mm <sup>-1</sup>
<i>F</i> (000)	2648
Crystal size	0.37 × 0.30 × 0.30 mm <sup>3</sup>
Theta range for data collection	3.03° to 27.49°
Limiting indices	$-18 \leq h \leq 12$ , $-19 \leq k \leq 17$ , $-33 \leq l \leq 33$
Reflections collected/unique	44028/12445 [ <i>R</i> <sub>int</sub> ] = 0.0309]
Completeness to $\theta = 27.49$	99.7%
Absorption correction	Empirical
Max. and min. transmission	0.5914 and 0.5337
Refinement method	Full-matrix least-squares on <i>F</i> <sup>2</sup>
Data/restraints/parameters	12445/0/721
Goodness-of-fit on <i>F</i> <sup>2</sup>	0.999
Final <i>R</i> indices [ <i>I</i> > 2σ( <i>I</i> )]	<i>R</i> <sub>1</sub> = 0.0289, <i>wR</i> <sub>2</sub> = 0.0683
<i>R</i> indices (all data)	<i>R</i> <sub>1</sub> = 0.0314, <i>wR</i> <sub>2</sub> = 0.0700
Largest diff. peak and hole	0.884 and -0.622 e Å <sup>-3</sup>

that of Nd–O bonds, which shows that the Nd–O bonds are stronger than Nd–N bonds.

Comparing with [Ln(BA)<sub>3</sub>bipy]<sub>2</sub> (Ln = Sm, Dy, and Eu), the average Ln–O bond distances are 2.385 Å for Sm, 2.364 Å for Eu, and 2.337 Å for Dy. The mean bond distances of Ln–N are 2.637 Å for Sm, 2.622 Å for Eu, and

**Fig. 1** Molecular structure of the title complex

2.583 Å for Dy. As expected, the average bond lengths of Ln–O (Ln = Nd, Sm, Dy, and Eu) and Ln–N both show a slight decrease from Nd<sup>3+</sup> to Eu<sup>3+</sup> ions, which may be explained by the lanthanide contraction.

#### Thermal decomposition of the complex

The TG/DTG curves of [Nd(BA)<sub>3</sub>bipy]<sub>2</sub> recorded at 15 K min<sup>-1</sup> are shown in Fig. 3. The data of the thermal decomposition are listed in Table 5. The first stage occurs from 415.76 to 541.12 K, with a mass loss of 23.25%, which corresponds to the loss of 2 mol bipy(theoretical mass loss : 23.53%). And it was confirmed by the disappearance of  $\nu_{\text{CN}}$  (1630 cm<sup>-1</sup>) in the IR spectra of the residue at 541.12 K.

Subsequently, in the range of 541.12–1085.36 K, the remaining undergoes the loss of BA ligands. The mass loss is 51.38%, which is in good agreement with the theoretical

**Table 4** Bond lengths [Å] and angles [°] for [Nd(BA)<sub>3</sub>bipy]<sub>2</sub>

Nd(1)–O(8)	2.3615(19)	Nd(1)–O(11)	2.4643(18)
Nd(1)–O(4)	2.3643(18)	Nd(1)–O(12)	2.5013(19)
Nd(1)–O(10)	2.3976(18)	Nd(1)–N(4)	2.640(2)
Nd(1)–O(6)	2.4254(18)	Nd(1)–N(3)	2.673(2)
O(8)–Nd(1)–O(11)	94.33(7)	O(9)–C(35)	1.259(3)
O(4)–Nd(1)–O(11)	147.28(6)	O(10)–C(35)	1.263(3)
O(10)–Nd(1)–O(11)	133.44(6)	O(8)–Nd(1)–O(12)	75.74(7)
O(6)–Nd(1)–O(11)	81.40(6)	O(4)–Nd(1)–O(12)	157.29(6)
O(11)–Nd(1)–O(12)	52.87(6)	O(10)–Nd(1)–O(12)	81.11(6)
O(8)–Nd(1)–N(4)	142.41(7)	O(6)–Nd(1)–O(12)	124.45(6)
O(4)–Nd(1)–N(4)	94.95(7)	O(8)–Nd(1)–O(4)	105.28(7)
O(10)–Nd(1)–N(4)	75.26(7)	O(8)–Nd(1)–O(10)	78.88(6)
O(12)–Nd(1)–N(4)	73.71(7)	O(4)–Nd(1)–O(10)	76.93(6)

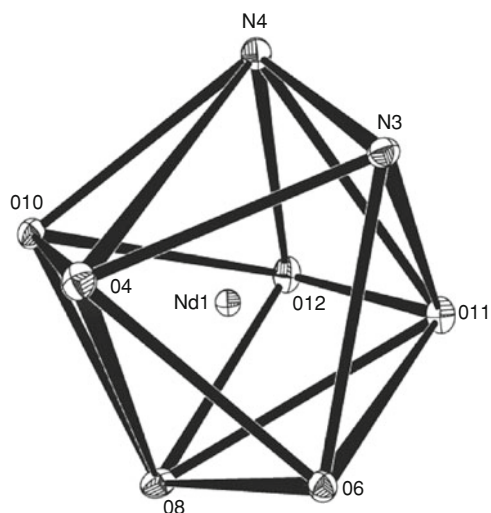


**Fig. 2** Coordination geometry of the  $\text{Nd}^{3+}$  ion

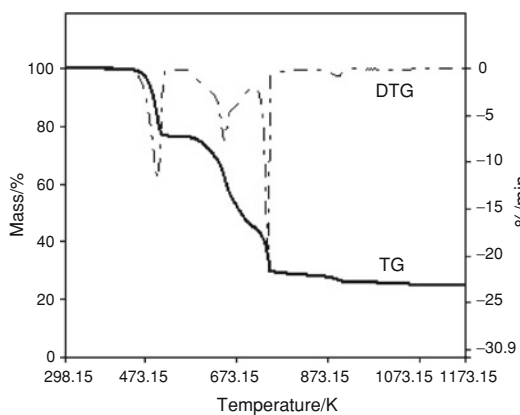
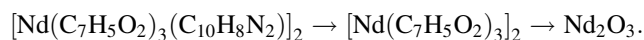


**Fig. 3** TG/DTG curves of  $[\text{Nd}(\text{BA})_3\text{bipy}]_2$  at a heating rate of  $15 \text{ K min}^{-1}$

value (51.12%). The characteristic absorption of the residue in IR spectra is the same as the standard sample spectra of  $\text{Nd}_2\text{O}_3$ . Therefore, the complex of  $[\text{Nd}(\text{BA})_3\text{bipy}]_2$  at 1085.36 K was completely degraded into  $\text{Nd}_2\text{O}_3$  with the total weight loss of 74.61% (theoretical mass loss: 74.65%). Based on the above analysis, the thermal

decomposition process of  $[\text{Nd}(\text{BA})_3\text{bipy}]_2$  may be described as follows:



Kinetics of the first decomposition stage

The integral isoconversional non-linear method [28] is used to calculate the activation energy  $E$  of the first decomposition stage. The relationship between  $E$  and  $\alpha$  is shown in Fig. 4. It can be seen that the values of  $E$  is of small variation with the whole decomposition process. This indicates that the first decomposition stage is a single step reaction [29]. So the probable mechanism function,  $E$  and  $A$  can be determined by means of double equal-double steps method.

Determination of  $f(\alpha)$  and  $G(\alpha)$

The Ozawa iteration equation [30] is as follows:

$$\ln \frac{\beta}{H(x)} = \left\{ \ln \left[ \frac{0.0048AE}{R} \right] - \ln G(\alpha) \right\} - 1.0516 \frac{E}{RT} \quad (1)$$

$$H(x) = \frac{\exp(-x)}{0.0048 \exp(-1.0516x)} h(x)$$

$$h(x) = \frac{x^4 + 18x^3 + 86x^2 + 96x}{x^4 + 20x^3 + 120x^2 + 240x + 120}$$

$$\ln G(\alpha) = \ln \left( \frac{0.0048AEH(x)}{R} \right) - 1.0516 \frac{E}{RT} - \ln \beta \quad (2)$$

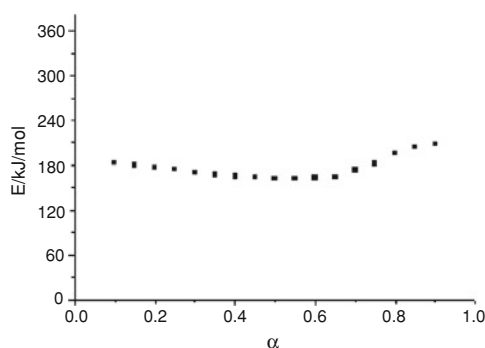


**Fig. 4** The relationship of  $E$  and  $\alpha$  of the first decomposition stage

**Table 5** Thermal decomposition data for  $[\text{Nd}(\text{BA})_3\text{bipy}]_2$  ( $\beta = 15 \text{ K min}^{-1}$ )

Temperature range/K	DTG peak temperature/K	Mass loss/%		Probable composition of removed groups	Intermediate
		TG	Theory		
415.76–541.12	508.15	23.25	23.53	$2\text{C}_{10}\text{H}_8\text{N}_2$	$[\text{Nd}(\text{C}_7\text{H}_5\text{O}_2)_3]_2$
541.12–1085.36	–	51.38	51.12	$(\text{C}_7\text{H}_5)_6\text{O}_9$	$\text{Nd}_2\text{O}_3$
		74.63 <sup>a</sup>	74.65 <sup>a</sup>		

<sup>a</sup> Total mass loss

where  $G(\alpha)$  is the integral mechanism function,  $T$  the absolute temperature,  $A$  the pre-exponential factor,  $R$  the gas constant,  $E$  the apparent activation energy,  $x$  the  $E/RT$ , and  $\beta$  the linear heating rate.

The values of  $\alpha$  at different heating rates and the same temperature on the TG/DTG curves of [Nd(BA)<sub>3</sub>bipy]<sub>2</sub> are shown in Table 6. By substituting the values of  $\alpha$ ,  $\beta$  in Table 6 and various conversion functions [31] into Eq. 2, using the linear least-squares method with  $\ln G(\alpha)$  vs.  $\ln \beta$ , the linear correlation coefficient  $r$ , the slope  $b$ , and the intercept  $a$  at different temperatures were obtained. Some results are listed in Table 7.

From Table 7, it can be concluded that only the coefficients  $r$  of the function no. 16 are best while the slope  $b$  is close to  $-1$ , so the probable mechanism function is

**Table 6** Conversion degrees measured for given the same temperatures on the TG/DTG curves of [Nd(BA)<sub>3</sub>bipy]<sub>2</sub> at different heating rates: stage 1

T/K	$\alpha$				
	$\beta = 3/$ K min <sup>-1</sup>	$\beta = 5/$ K min <sup>-1</sup>	$\beta = 10/$ K min <sup>-1</sup>	$\beta = 12/$ K min <sup>-1</sup>	$\beta = 15/$ K min <sup>-1</sup>
473.44	0.4787	0.3116	0.1786	0.1351	0.1249
475.71	0.5601	0.3784	0.2138	0.1661	0.1507
477.71	0.6286	0.4407	0.2526	0.1977	0.1764
479.38	0.6720	0.4988	0.2874	0.2262	0.2010
481.04	0.7051	0.5598	0.3262	0.2582	0.2288

**Table 7** Some results from the linear least-squares method at different temperatures for [Nd(BA)<sub>3</sub>bipy]<sub>2</sub>: stage 1

T/K	Function no.*	$a$	$b$	$r$
473.44	16	0.286524	-1.00774	-0.996582
	26	0.136607	-1.28716	-0.996463
	37	0.504280	-1.17732	-0.995741
475.71	16	0.399582	-1.02741	-0.997753
	26	0.233014	-1.25988	-0.997328
	37	0.679362	-1.24672	-0.996704
477.71	16	0.487741	-1.03435	-0.998322
	26	0.294346	-1.21645	-0.997132
	37	0.831067	-1.30410	-0.997331
479.38	16	0.542971	-1.02414	-0.998153
	26	0.322559	-1.16230	-0.995454
	37	0.937511	-1.33277	-0.998156
481.04	16	0.582535	-0.998693	-0.996555
	26	0.332406	-1.09227	-0.991898
	37	1.02542	-1.34162	-0.998167

\* The function No. is from Tables 6–10 in [31]

$G(\alpha) = -\ln(1 - \alpha)$ ,  $f(\alpha) = (1 - \alpha)$ . The first stage of the decomposition mechanism is controlled by assumed random nucleation and its subsequent growth ( $n = 1$ ). The kinetic equation of this stage can be expressed as  $d\alpha/dt = A \exp(-E/RT)(1 - \alpha)$ .

Calculation of  $E$  and  $A$

The value of activation energy is calculated by Ozawa iteration method by substituting the values of  $\alpha$ ,  $\beta$ , and  $T$  in Table 8 and the corresponding mechanism function no. 16 into Eq. 1, via the linear least-squares method with  $\ln \beta/H(x)$  vs.  $1/T$ . The activation energy  $E$  can be calculated from the value of the slope and the pre-exponential factor  $A$  can also be calculated from the value of the intercept. The results are listed in Table 9.

The thermodynamic parameters of activation can be calculated from the equations [32, 33]:

$$A \exp(-E/RT) = \nu \exp(-\Delta G^\ddagger/RT) \tag{3}$$

$$\Delta H^\ddagger = E - RT \tag{4}$$

$$\Delta G^\ddagger = \Delta H^\ddagger - T\Delta S^\ddagger \tag{5}$$

where  $\nu$  is the Einstein vibration frequency,  $\Delta G^\ddagger$  is the Gibbs free enthalpy of activation,  $\Delta H^\ddagger$  is the enthalpy of activation,  $\Delta S^\ddagger$  is entropy of activation. The values of entropy, enthalpy, and the Gibbs free energy of activation

**Table 8** The values of temperatures at the same degree of conversion for the different heating rate on TG/DTG curves for the title complex (stage 1)

$\alpha$	T/K				
	$\beta = 3/$ K min <sup>-1</sup>	$\beta = 5/$ K min <sup>-1</sup>	$\beta = 10/$ K min <sup>-1</sup>	$\beta = 12/$ K min <sup>-1</sup>	$\beta = 15/$ K min <sup>-1</sup>
0.10	456.13	460.49	466.47	469.73	470.72
0.15	460.52	465.00	471.38	474.47	475.70
0.20	463.50	468.24	474.82	477.84	479.32
0.25	466.02	470.83	477.59	480.63	482.24
0.30	467.94	473.02	479.92	483.03	484.71
0.35	469.69	474.78	481.86	485.05	486.86
0.40	471.28	476.42	483.76	486.89	488.74
0.45	472.73	477.96	485.34	488.48	490.53
0.50	474.02	479.41	486.84	490.02	492.18
0.55	475.43	480.78	488.28	491.50	493.74
0.60	476.92	482.00	489.62	492.84	495.20
0.65	478.45	483.22	490.94	494.21	496.59
0.70	480.83	484.53	492.13	495.41	497.97
0.75	482.91	486.09	493.37	496.69	499.40
0.80	484.59	488.86	494.60	497.96	500.65
0.85	486.21	491.19	495.99	499.35	502.08
0.90	487.83	493.63	497.38	500.85	503.75

**Table 9** The values of the kinetic parameters computed by the ozawa iteration method

$\alpha$	$A \times 10^{17}/\text{min}^{-1}$	$E/\text{kJ mol}^{-1}$	$r$
0.10	30.81457	183.634	-0.996066
0.15	13.57439	180.717	-0.997269
0.20	52.07461	177.096	-0.998057
0.25	30.77541	175.106	-0.998201
0.30	10.85934	171.050	-0.998369
0.35	5.57895	168.405	-0.998319
0.40	3.42685	166.456	-0.998566
0.45	2.48020	165.123	-0.998685
0.50	1.58038	163.277	-0.998752
0.55	1.47244	162.937	-0.998642
0.60	1.90260	163.879	-0.998287
0.65	2.80468	165.355	-0.997602
0.70	27.78299	174.499	-0.993833
0.75	19.69458	182.357	-0.990678
0.80	64.76541	196.477	-0.993297
0.85	43.66632	204.208	-0.991983
0.90	12.69539	208.489	-0.985909
	30.6703 <sup>av</sup>	177.004 <sup>av</sup>	

av average value of  $E$  and  $A$

**Table 10** The thermodynamic parameters of the title complex

$\beta/$ $\text{K min}^{-1}$	$\Delta H^\ddagger/$ $\text{kJ mol}^{-1}$	$\Delta G^\ddagger/$ $\text{kJ mol}^{-1}$	$\Delta S^\ddagger/$ $\text{J mol}^{-1} \text{K}^{-1}$	$T_p/\text{K}$
3	173.03	126.77	96.76	478.12
5	172.99	126.27	96.67	483.27
10	172.90	125.30	96.50	493.27
12	172.87	124.90	96.43	497.43
15	172.85	124.66	96.39	499.88

at the peak temperature acquired on the basis of Eqs. 3–5 are listed in Table 10. As seen in Table 10, the values of  $\Delta G^\ddagger > 0$ , indicating that the decomposition reactions for the title complex were not spontaneous reactions.

## Conclusions

The crystal structure of  $[\text{Nd}(\text{BA})_3\text{bipy}]_2$  was determined by single crystal X-ray diffraction. The crystal is monoclinic with space group  $P2(1)/n$  and the coordination number of  $\text{Nd}^{3+}$  ion is eight. The mechanism function of the first stage for the complex is  $G(\alpha) = -\ln(1 - \alpha)$ ,  $f(\alpha) = 1 - \alpha$ . The kinetic equation of this stage can be expressed as  $dx/dt = A \exp(-E/RT)(1 - \alpha)$ . The activation energy  $E$  and the pre-exponential factor  $A$  are  $177.004 \text{ kJ mol}^{-1}$ ,  $30.6703 \times 10^{17} \text{ min}^{-1}$ , respectively. And the enthalpy of

activation  $\Delta H^\ddagger$ , the Gibbs free energy of activation  $\Delta G^\ddagger$ , and the entropy of activation  $\Delta S^\ddagger$  were also obtained.

## Supplementary material

CCDC: 711420 contains the supplementary crystallographic data for this paper. These data can be obtained free of charge via <http://www.ccdc.cam.ac.uk/conts/retrieving.html>, or from the Cambridge Crystallographic Data Centre, 12 Union Road, Cambridge CB2 1EZ, UK (fax: int.code +(1223)336-0333; e-mail for inquiry: fileserv@ccdc.cam.ac.uk).

**Acknowledgements** This project was supported by the National Natural Science Foundation of China (No. 20773034) and the Natural Science Foundation of Hebei Province (No. B2007000237).

## References

- Li X, Zhang ZY, Zou YQ. Synthesis, structure and luminescence properties of four novel terbium 2-fluorobenzoate complexes. *Eur J Inorg Chem.* 2005; 2909–918.
- Song YS, Yan B, Weng LH. Four distinctive 1-D lanthanide carboxylate coordination polymers: synthesis, crystal structures and spectral properties. *Polyhedron.* 2007;26:4591–601.
- Huang Y, Yan B, Shao M. Synthesis, crystal structure and photoluminescent properties of four lanthanide 5-nitroisophthalate coordination polymers. *J Solid State Chem.* 2009;182:657–68.
- Zhao LY, Chen YP, Zhang HH, Li CY, Sun RQ, Yang QY. Study of structure and two-dimension correlation infrared spectroscopy on three rare-earth/3-methylbenzoic acid complexes. *J Mol Struct.* 2009;920:441–9.
- Deng H, Cai YP, Chao H. Synthesis, characterization and crystal structures of lanthanide phenoxyacetate complexes with 1, 10-phenanthroline. *Chin J Inorg Chem.* 2003;21:409–14.
- Thompson L, Legendziewicz J, Cybinska J, Li P, Brennessel W. Structure, photophysics and magnetism of a europium mixed complex  $\text{Eu}(\text{HFAA})_3\text{bipy}\cdot\text{H}_2\text{O}$  in the solid state and solution. *J Alloy Compd.* 2002;341:312–22.
- Yang YT, Zhan SY. Study of lanthanide complexes with salicylic acid by photoacoustic and fluorescence spectroscopy. *Spectrochim Acta A.* 2004;60:2065–9.
- Huang CH. Coordination chemistry of rare earths. Beijing: Science Press; 1997. p. 378–87.
- Zhang HY, Ren N, Tian L, Zhang JJ. Thermal decomposition reaction kinetics of complexes of  $[\text{Sm}(\text{o-MOBA})_3\text{bipy}]_2\cdot\text{H}_2\text{O}$  and  $[\text{Sm}(\text{m-MOBA})_3\text{bipy}]_2\cdot\text{H}_2\text{O}$ . *J Therm Anal Calorim.* doi:10.1007/s10973-009-0304-0.
- Ren N, Zhang JJ, Wang RF. Synthesis, crystal structure and thermal decomposition process of complex  $[\text{Sm}(\text{BA})_3\text{phen}]_2$ . *J Chil Chem Soc.* 2006;53:293–8.
- Ren N, Zhang JJ, Guo YH, Sun MQ, Xu SL, Zhang HY. Non-isothermal decomposition kinetics of complexes  $[\text{Sm}(\text{m-MBA})_3\text{phen}]_2$  and  $[\text{Sm}(\text{o-MOBA})_3\text{phen}]_2\cdot 2\text{H}_2\text{O}$ . *Chem Res Chin U.* 2007;23:489–92.
- Ionashiro EY, Bannach G, Siqueira AB, deCarvalho CT, Rodrigues EC, Ionashiro M. 2-Methoxybenzylidenepyruvate with

- heavier trivalent lanthanides and yttrium(III) synthesis and characterization. *J Therm Anal Calorim.* 2008;92:953–9.
13. Zhang JJ, Xu SL, Ren N, Zhang HY, Tian L. Preparation and thermal decomposition reaction kinetics of a dysprosium(III) p-chlorobenzoate 1, 10-phenanthroline complex. *Int J Chem Kinet.* 2008;40:66–72.
  14. Ferenc W, Dziewulska-Kuackowska A, Sarzynski J, Paszkowska B. 4-Chloro-2-methoxybenzoates of heavy lanthanides(III) and yttrium(III) thermal spectral and magnetic behaviour. *J Therm Anal Calorim.* 2008;91:285–92.
  15. Zhang JJ, Ren N, Bai JH, Xu SL. Synthesis and thermal decomposition reaction kinetics of complexes of [Sm<sub>2</sub>(*m*-CIBA)<sub>6</sub>(phen)<sub>2</sub>·2H<sub>2</sub>O and [Sm<sub>2</sub>(*m*-BrBA)<sub>6</sub>(phen)<sub>2</sub>·2H<sub>2</sub>O]. *Int J Chem Kinet.* 2007;39:67–74.
  16. Locatelli JR, Rodrigues EC, Siqueira AB, Ionashiro EY, Bannach G, Ionashiro M, et al. Synthesis, characterization and thermal behaviour of solid-state compounds of yttrium and lanthanide benzoates. *J Therm Anal Calorim.* 2007;90(3):737–46.
  17. Xu XL, Zhang JJ, Yang HF, Ren N, Zhang HY. Synthesis, crystal structure and thermal decomposition of a dysprosium(III) p-fluorobenzoate 1, 10-phenanthroline complex. *J Chem Sci.* 2007; 62b:51–4.
  18. Zhang HY, Zhang JJ, Ren N, Xu SL, Tian L, Bai JH. Synthesis, crystal structure and thermal decomposition mechanism of the complex [Sm(*p*-BrBA)<sub>3</sub>bipy·H<sub>2</sub>O]<sub>2</sub>·H<sub>2</sub>O. *J Alloy Compd.* 2008; 464:277–81.
  19. Tian L, Ren N, Zhang JJ, Liu HM, Bai JH, Ye HM, et al. Synthesis, crystal structure luminescence and thermal decomposition kinetics of Eu(III) complex with 2, 4-dichlorobenzoic acid and 2, 2'-bipyridine. *Inorg Chim Acta.* 2009;362:3388–94.
  20. Zhang JJ, Ren N. A new kinetic method of processing TA data. *Chin J Chem.* 2004;22:1459–62.
  21. Shi YZ, Sun XZ, Jiang YH. Spectra and chemical identification of organic compounds. Nanjing: Science and Technology Press; 1988. p. 98.
  22. Xu CJ, Xie F, Guo XZ, Yang H. Synthesis and cofluorescence of Eu(Y) complexes with salicylic acid and o-phenanthroline. *Spectrochim Acta A.* 2005;61:2005–8.
  23. Wang RF, Jin LP, Wang MZ, Huang SH, Chen XT. Synthesis, crystal structure and luminescence of coordination compound of europium p-methylbenzoate with 2, 2'-dipyridine. *Acta Chimica Sinica.* 1995;53:39–45.
  24. Zhang HY, Wu KZ, Zhang JJ. Synthesis, crystal structure and thermal decomposition kinetics of the complex [Sm(BA)<sub>3</sub>bipy]<sub>2</sub>. *Synth Met.* 2008;158:157–64.
  25. Tian L, Ren N, Zhang JJ, Sun SJ, Ye HM, Bai JH, et al. Synthesis, crystal structure, and thermal decomposition kinetics of the complex of dysprosium benzoate with 2, 2'-bipyridine. *J Chem Eng Data.* 2009;54:69–74.
  26. Zhang Y, Jin LP, Lü SZ. Crystal structure and luminescence of [Eu<sub>2</sub>(BA)<sub>6</sub>(bipy)<sub>2</sub>]. *J Inorg Chem (in Chinese).* 1997;13:280–7.
  27. Lam AWH, Wong WT, Gao S, Wen GH, Zhang XX. Synthesis, crystal structure, and photophysical and magnetic properties of dimeric and polymeric lanthanide complexes with benzoic acid and its derivatives. *Eur J Inorg Chem.* 2003; 149–63.
  28. Vyazovkin S, Dollimore D. Linear and nonlinear procedures in isoconversional computations of the activation energy of non-isothermal reactions in solids. *J Chem Inf Comput Sci.* 1996; 36:42–5.
  29. Lu ZR, Ding YC, Xu Y, Li BL, Zhang Y. TA Study on four-one-dimensional chain copper complexes with benzoylacetone or 1, 1, 1-trifluoro-3-(2-thenoyl)-acetone bridged through azobispyridine ligands. *J Inorg Chem (in Chinese).* 2005;21:181–5.
  30. Gao Z, Nakada M, Amasski I. A consideration of errors and accuracy in the isoconversional methods. *Thermochim Acta.* 2001;369:137–42.
  31. Hu RZ, Gao SL, Zhao FQ, Shi QZ, Zhang TL, Zhang JJ. Thermal analysis kinetics. 2nd ed. Beijing: Science Press; 2008. p. 151.
  32. Straszko J, Olstak-Humienik M, Mozejko J. Kinetics of thermal decomposition of ZnSO<sub>4</sub>·7H<sub>2</sub>O. *Thermochim Acta.* 1997;292: 145–50.
  33. Olstak-Humienik M, Mozejko J. Thermodynamic functions of activated complexes created in thermal decomposition processes of sulphates. *Thermochim Acta.* 2000;344:73–9.